

# Biologically Guided Optimization of Test Target Location for Rod-mediated Dark Adaptation in Age-related Macular Degeneration

## Alabama Study on Early Age-related Macular Degeneration 2 Baseline

Cynthia Owsley, PhD, MSPH,<sup>1</sup> Thomas A. Swain, MPH,<sup>1,2</sup> Gerald McGwin, Jr., PhD, MS,<sup>1,2</sup>  
Mark E. Clark, MEng,<sup>1</sup> Deepayan Kar, MS,<sup>1</sup> Christine A. Curcio, PhD<sup>1</sup>

**Purpose:** We evaluate the impact of test target location in assessing rod-mediated dark adaptation (RMDA) along the transition from normal aging to intermediate age-related macular degeneration (AMD). We consider whether RMDA slows because the test locations are near mechanisms leading to or resulting from high-risk extracellular deposits. Soft drusen cluster under the fovea and extend to the inner ring of the ETDRS grid where rods are sparse. Subretinal drusenoid deposits (SDDs) appear first in the outer superior subfield of the ETDRS grid where rod photoreceptors are maximal and spread toward the fovea without covering it.

**Design:** Cross-sectional.

**Participants:** Adults  $\geq 60$  years with normal older maculas, early AMD, or intermediate AMD as defined by the Age-Related Eye Disease Study (AREDS) 9-step and Beckman grading systems.

**Methods:** In 1 eye per participant, RMDA was assessed at 5° and at 12° in the superior retina. Subretinal drusenoid deposit presence was identified with multi-modal imaging.

**Main Outcome Measures:** Rod intercept time (RIT) as a measure of RMDA rate at 5° and 12°.

**Results:** In 438 eyes of 438 persons, RIT was significantly longer (i.e., RMDA is slower) at 5° than at 12° for each AMD severity group. Differences among groups were bigger at 5° than at 12°. At 5°, SDD presence was associated with longer RIT as compared to SDD absence at early and intermediate AMD but not in normal eyes. At 12°, SDD presence was associated with longer RIT in intermediate AMD only, and not in normal or early AMD eyes. Findings were similar in eyes stratified by AREDS 9-step and Beckman systems.

**Conclusions:** We probed RMDA in relation to current models of deposit-driven AMD progression organized around photoreceptor topography. In eyes with SDD, slowed RMDA occurs at 5° where these deposits typically do not appear until later in AMD. Even in eyes lacking detectable SDD, RMDA at 5° is slower than at 12°. The effect at 5° may be attributed to mechanisms associated with the accumulation of soft drusen and precursors under the macula lutea throughout adulthood. These data will facilitate the design of efficient clinical trials for interventions that aim to delay AMD progression. *Ophthalmology Science* 2023;3:100274 © 2023 by the American Academy of Ophthalmology. This is an open access article under the CC BY-NC-ND license (<http://creativecommons.org/licenses/by-nc-nd/4.0/>).



Supplemental material available at [www.opthalmologyscience.org](http://www.opthalmologyscience.org).

Age-related macular degeneration (AMD) is a globally prevalent disease of aging that is managed medically in the 15% of patients with exudative complications and lacks a targeted treatment for the remaining 85%. Initial trial results for inhibitors of complement cascade proteins, the largest pathway implicated by genetics, show promise in slowing the expansion of atrophy.<sup>1–3</sup> Treatments at earlier stages of

disease, before irreversible tissue and visual damage, remain a research priority.

A 1993 cross-sectional study from Bird's group noted that rod-mediated dark adaptation (RMDA), a functional test of retinoid resupply to photoreceptors from circulation, was slow in patients with early AMD.<sup>4</sup> In the early 2000s, using fundus grading to characterize macular health, we showed

that RMDA worsened from normal aging to early and intermediate AMD.<sup>5,6</sup> Many groups have replicated these findings and extended them by demonstrating that delayed RMDA is associated with structural perturbations in retina.<sup>7–18</sup> The prospective Alabama Study on Age-Related Macular Degeneration showed that the first functional biomarker for incident early AMD was delayed RMDA. Older adults in normal macular health and slow RMDA at baseline were 2 times more likely to have early AMD 3 years later than those with normal RMDA.<sup>19</sup> Performance on cone-mediated tasks was unrelated to incident AMD.<sup>20</sup> Furthermore, delayed RMDA in normal older adults was associated with one of the strongest AMD risk genes, age-related maculopathy susceptibility 2 (*ARMS2*).<sup>21</sup>

Ideally, clinical trial outcomes should meaningfully impact vision by preventing, halting, or reversing the disease process. In addition to choosing functional tests that reflect activity along causal pathways in AMD progression, test characteristics like repeatability and instrument availability are important practical considerations for designing a functional test. To enhance our ability to detect RMDA slowing and maximize the effect as an outcome, we herein optimize the retinal eccentricity of the test target. Several research groups reported that sensitivity recovery by rods was slowest at 3° to 5° compared to more eccentric locations,<sup>12,13,22,23</sup> without suggesting a biologic basis for this finding.<sup>18</sup> We found that modulators of rod intercept time (RIT) rate localized to outer retinal reflective bands at 1.7° (0.5 mm) and not at 6.9° (2 mm).<sup>18</sup> Sharply declining gradients in photoreceptor density are deployed in a radially symmetric fashion from the foveal center. Thus, test targets a few degrees apart stimulate markedly different numbers of cones, rods, and support cells (Fig 1A, B). Locations close to the fovea with poor RMDA have low rod:cone ratio (~3–10 at 4°–5°). More eccentric locations with better performance have higher rod:cone ratio (~10–15 at 6°–12°).

The current study seeks to evaluate regional differences in RMDA rate, using test target locations at 5° and 12° superior to the fovea. We were guided by a model of AMD pathophysiology, in which 2 layers of extracellular deposits related to cone and rod topography each presage distinct end-stages of neovascularization and atrophy (Fig 1A).<sup>30,31</sup> High-risk drusen cluster under the fovea and extend to the inner ring of the ETDRS grid, mirroring foveal cones, specialized glia, and xanthophyll pigment. Subretinal drusenoid deposit (SDD; also called reticular pseudodrusen) appear first within the outer superior sub-field of the ETDRS grid where rod photoreceptors are maximal and spread toward the fovea without covering it. Thus, poor RMDA may be due to the proximity of the test location to mechanisms leading to and resulting from high-risk deposits.

To explore the basis of regional differences in RMDA, the current study tested RMDA at both 5°, where rods are sparse and the dominant deposit is soft drusen material, and at 12°, where rods are numerous, and the dominant deposit is SDD. Unlike earlier studies of RMDA test target location that used small samples (23–65 eyes),<sup>12,13,22,23</sup> the current study

includes a large sample (N = 438) of older adults in normal macular health and with early and intermediate AMD.

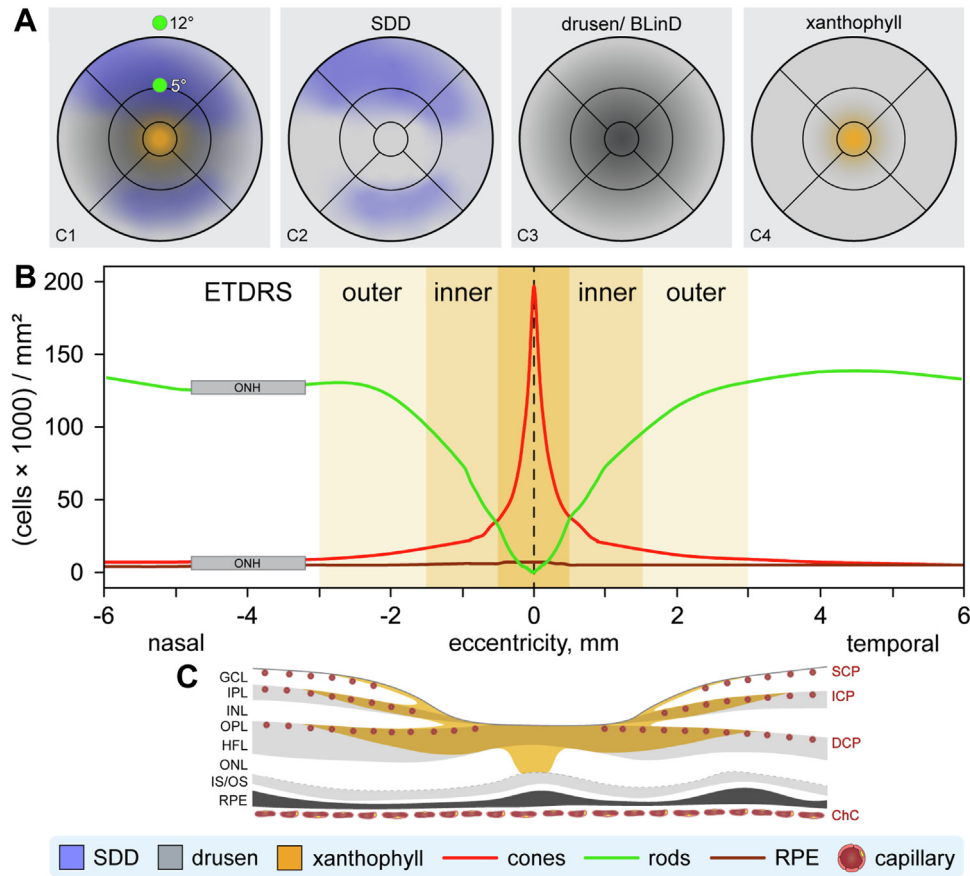
## Methods

The Alabama Study on Early Age-Related Macular Degeneration 2 (ALSTAR2) is a prospective cohort study on normal aging and early and intermediate AMD whose purpose is to validate retinal imaging characteristics in these conditions with visual function (Clinicaltrials.gov identifier NCT04112667, October 7, 2019). The study was approved by the Institutional Review Board of the University of Alabama at Birmingham. All participants provided written informed consent after the nature and purpose of the study were explained. Conduct of the study followed the Declaration of Helsinki. The baseline data from ALSTAR2 were collected between October 2019 and September 2021, which included a 4-month pause in enrollment due to the coronavirus disease 2019 pandemic (March–June 2020).

Participants ≥ 60 years old were recruited from the Callahan Eye Hospital Clinics, the clinical service of the University of Alabama at Birmingham Department of Ophthalmology and Visual Sciences. We recruited 3 groups—those with early AMD and intermediate AMD, and those in normal macular health. The clinic's electronic health record was used to search for patients with early or intermediate AMD using International Classification of Diseases 10 codes (H35.30\*; H35.31\*; H35.36\*). One of the investigators (C.O.) screened charts to confirm that participants met the eligibility criteria. Exclusion criteria were (1) any eye condition or disease in either eye (other than early cataract) in the medical record that can impair vision including diabetic retinopathy, glaucoma, ocular hypertension, history of retinal diseases (e.g., retinal vein occlusion, retinal degeneration), optic neuritis, corneal disease, previous ocular trauma or surgery, refractive error ≥ 6 diopters; (2) neurological conditions that can impair vision or judgment including multiple sclerosis, Parkinson's disease, stroke, Alzheimer's disease, seizure disorders, brain tumor, traumatic brain injury; (3) psychiatric disorders that could impair the ability to follow directions, answer questions about health and functioning, or to provide informed consent; (4) diabetes; (5) any medical condition that causes significant frailty or was thought to be terminal. Persons in normal macular health met the same eligibility criteria except they did not have International Classification of Diseases 10 codes indicative of AMD. Letters were sent to potential participants, with the study coordinator following up by phone to determine interest.

One eye was tested for each participant, with the eye selected for testing being the eye with better acuity. If the eyes had the same acuity, then an eye was randomly selected. Classification into the 3 groups was based on a trained grader's (M.E.C.) evaluation of 3-field color fundus photographs taken with a digital camera (450+, Carl Zeiss Meditec) following dilation with 1% tropicamide and 2.5% phenylephrine hydrochloride. The Age-Related Eye Disease Study (AREDS) 9-step classification system<sup>32</sup> was used by the grader to identify AMD presence and severity, and group membership was determined, as follows: eyes in normal macular health had AREDS grade 1, early AMD had grades 2 to 4, and intermediate AMD had grades 5 to 8. We also used the Beckman classification system<sup>33</sup> with normal aging as grades 1 to 2, early AMD as grade 3, and intermediate AMD as grade 4. The grader was masked to all other participant characteristics. As described,<sup>14</sup> intragrader agreement was  $K = 0.88$ ; intergrader agreement with a second grader was  $K = 0.75$ .

Demographic information for birthdate, gender, and race/ethnicity was obtained through self-administered questionnaire.



web 4C/FPO

**Figure 1.** Center-surround model of vision function testing and deposit-driven age-related macular degeneration (AMD) progression. This study tests the hypothesis that rod-mediated dark adaptation (RMDA) will be poor (slower) at test locations affected by mechanisms leading to and resulting from extracellular deposits with high risk for AMD progression, viz., soft drusen and subretinal drusenoid deposit (SDD). **A1–4**, Locations of test targets and AMD deposits, shown on an ETDRS grid. **A1**, The test target locations are 5° and 12° superior to the fovea. Blue indicates SDD,<sup>24</sup> also shown alone in **(A2)**. Gray indicates soft drusen material,<sup>25</sup> also shown alone in **(A3)**. **A2**, At 12° SDD is dominant, and rods are numerous. **A3**, At 5°, soft drusen and basal linear deposit are dominant, and rods are sparse. **A4**, Xanthophyll carotenoids are abundant in the central subfield of ETDRS grid and reduced in the inner ring. **B**, Spatial density of cone and rod inner segments and retinal pigment epithelium (RPE) in human retina.<sup>26,27</sup> Shades of yellow indicate subfields of the ETDRS grid. Central subfield and inner ring exhibit the highest and next-highest population-level risk for AMD progression.<sup>28</sup> Together these are coterminous with the macula lutea, containing the highest concentration of xanthophyll pigment, in **(C)**. **C**, Cross-section of central macula showing xanthophyll carotenoid pigment concentrated in the foveal center with extensions into the plexiform layers and nerve fiber layer.<sup>15,29</sup> Foveal cones are protected by specialized Müller glia that harbor these pigments and access nutrients and oxygen via the retinal circulation. BLinD = basal linear deposit; ChC = choriocapillaris; DCP = deep capillary plexus; GCL = ganglion cell layer; HFL = Henle fiber layer; ICP = intermediate capillary plexus; INL = inner nuclear layer; IPL = inner plexiform layer; IS = inner segment; ONL = outer nuclear layer; OPL = outer plexiform layer; OS = outer segment; SCP = superficial capillary plexus.

Rod-mediated dark adaptation was assessed with the AdaptDx (MacuLogix). Testing occurred in a dark, light-tight room after dilation. Dark adaptation was measured with targets at 2 locations on the superior vertical meridian of retina, run in separate protocols separated by approximately 60 minutes: 5° eccentricity to probe the area of proportionately greatest rod loss in aging and AMD<sup>34,35</sup> and 12° eccentricity to probe the area of highest rod density.<sup>34</sup> The order of RMDA testing for each target location was randomly determined for each participant. The procedure began with a photo-bleach exposure to a 6° diameter flash centered at each test target location (equivalent ~83% bleach; 50 ms duration, 58 000 scotopic cd/m<sup>2</sup> s intensity<sup>36</sup>) while the participant focused on the fixation light. Threshold measurement (3-down/1 up threshold strategy) for a 2° diameter, 500 nm circular target began 15 seconds after bleach offset. The participant was instructed to maintain fixation and press a button when the flashing target first became visible. Log thresholds were expressed as sensitivity in

decibel units as a function of time since bleach offset. Threshold measurement continued at 30-second intervals until the RIT was reached. Rod intercept time is the duration in minutes required for sensitivity to recover to a criterion value of  $5.0 \times 10^{-3}$  scotopic cd/m<sup>2</sup>,<sup>19,37</sup> located in the latter half of the second component of rod-mediated recovery.<sup>38,39</sup> If RIT was not reached, the threshold measurement procedure stopped at 45 minutes. For some participants where the threshold measurement procedure was stopped, the AdaptDx's algorithm generated a RIT if it could be computed based on previous thresholds. Participants with fixation errors > 30% were excluded from analysis.

Prompted by evidence that SDD accentuate RMDA delays,<sup>7–9</sup> we also examined RMDA at 5° and 12° locations comparing eyes with SDD and eyes with no detectable SDD. As described,<sup>40</sup> SDD presence was identified using multimodal imaging in 2 steps. An initial screening step utilized near infrared reflectance and *en face* OCT using Spectralis HRA + OCT (Heidelberg

Engineering). In near infrared reflectance imaging, SDD lesions had to be visible as either solid or annular hyporeflective lesions in a distinct punctate pattern.<sup>41</sup> *En face* OCT slabs were generated by setting the top boundary at the external limiting membrane band and the lower boundary at the interdigitation zone band. In these slabs SDD had to be visible as a patchy hyperreflective pattern or solitary hyperreflective lesions each surrounded by a hyporeflective annulus. Once SDD was visible on either near infrared reflectance or *en face* OCT,  $\geq 5$  definite accumulations above the retinal pigment epithelium (RPE) in  $> 1$  B-scan on cross-sectional OCT were required for confirming SDD presence.<sup>41</sup> These assessments were made by a grader (D.K.) masked to all visual function characteristics. A second grader (M.E.C.), also masked to visual function, assessed a random 14% sub-sample of study eyes. Agreement with the first grader on the presence of SDD was strong (Cohen's  $\kappa = 0.89$ , 95% confidence interval 0.77–1.0).

## Statistical Analysis

Continuous and categorical data were summarized using means and standard deviations or number and percent. Rod intercept time at 5° and 12° by AMD severity category were compared using analysis of covariance with pairwise comparisons for all eyes testing for interaction between SDD presence and AMD severity. All models were age-adjusted. Rod intercept time at 5° and 12° was compared for all eyes using a paired t-test. At each target location, we also compared eyes with SDD to eyes with no SDD stratified by AMD status with analysis of covariance adjusted for age. The frequency of invalid tests at each location was compared using a chi-square test. The significance level for all analyses was  $P \leq 0.05$  (2-sided). Analyses were completed in SAS version 9.4 (SAS Institute).

## Results

A total of 438 eyes from 438 participants had RMDA tested at both 5° and 12°. Table S1 (available at <https://www.opthalmologyscience.org>) shows the demographic characteristics of the sample. Approximately 91% of participants were between 60 and 79 years old. Eyes with SDD were from persons on average older than eyes with no SDD (SDD: mean age 73.4 (5.7); No SDD: mean age 71.2 (6.1),  $P = 0.0014$ ). Using the AREDS 9-step system, persons with intermediate AMD were on average older than persons with normal eyes and those with early AMD ( $P < 0.0001$ ). About 2/3 of the sample was female and  $> 90\%$  were white of European descent.

Figure 2 compares RIT at 5° and 12° for each participant in a scatter plot. This analysis demonstrates that across the spectrum of measurements, RIT at 5° was longer than 12° ( $P < 0.0001$ ). This figure also shows that the difference between 5° and 12° widened with greater AMD. Thus, for RIT values  $< 9.5$  minutes, there were more normal and early AMD eyes and no intermediate AMD eyes. At the longest RIT for RMDA 5° ( $\geq 45$  minutes), RIT for RMDA 12° was highly variable.

When eyes are stratified by the AREDS 9-step system, RIT is significantly longer (i.e., RMDA is slower) at 5° than at 12° for each AMD severity group ( $P < 0.0001$  in each individual group), as shown in Figure 3. As illustrated in Fig S4 (available at <https://www.opthalmologyscience.org>), we also found a significant interaction for RIT between eyes

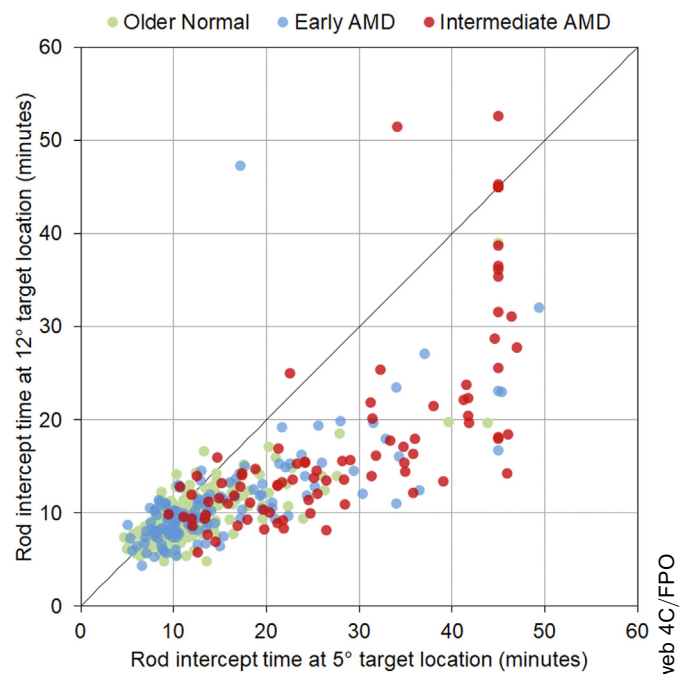


**Figure 2.** Scatter plot showing rod intercept time (RIT) at 5° and 12° for each participant stratified by Age-Related Eye Disease Study (AREDS) 9-step age-related macular degeneration (AMD) severity. The identity line represents a hypothetical scenario in which rod-mediated dark adaptation (RMDA) 5° and RMDA 12° are equal ( $x = y$ , slope = 1) in each participant. The majority had longer RITs at 5° compared to 12°. RIT for RMDA 5° in intermediate AMD eyes is  $\geq 9.5$  minutes, whereas RIT in many older normal and early AMD eyes is  $< 9.5$ .

with SDD versus no SDD and AMD severity group for 5° ( $P = 0.0012$ ) and 12° ( $P < 0.0001$ ). At 5° SDD presence is associated with greater RIT for SDD as compared to SDD absent at both early and intermediate AMD. There was no difference in RIT for SDD presence versus SDD absence in normal older eyes. At 12° SDD presence was associated with greater RIT at intermediate AMD only, and not in normal older eyes or in early AMD. Among all participants, RIT at both 5° and 12° increased with AMD severity (Table 2). When comparing by AMD severity, at 5° eyes in normal macular health were significantly faster than eyes with early and intermediate AMD ( $P = 0.0008$  and  $P < 0.0001$ , respectively) and early AMD faster than intermediate AMD ( $P < 0.0001$ ). Results were similar for 12°, except that normal eyes did not differ from early AMD eyes ( $P = 0.0678$ ). When stratified by SDD status, RIT was significantly faster at both 5° and 12° among eyes without SDD than in eyes with SDD. Among eyes with SDD, RIT did not differ in normal eyes compared to those with early AMD at 5° and 12° but did for normal eyes versus intermediate and early versus intermediate eyes. At 5°, 6.9% of the sample had fixation errors exceeding 30%, indicating the data are invalid and could not be used. The frequency of invalid tests at 12° was 10.6%, significantly higher than 5° ( $P < 0.0001$ ).

We next report the results using the Beckman classification system, in Figs S5 and S6, analogous to Figure 3 and

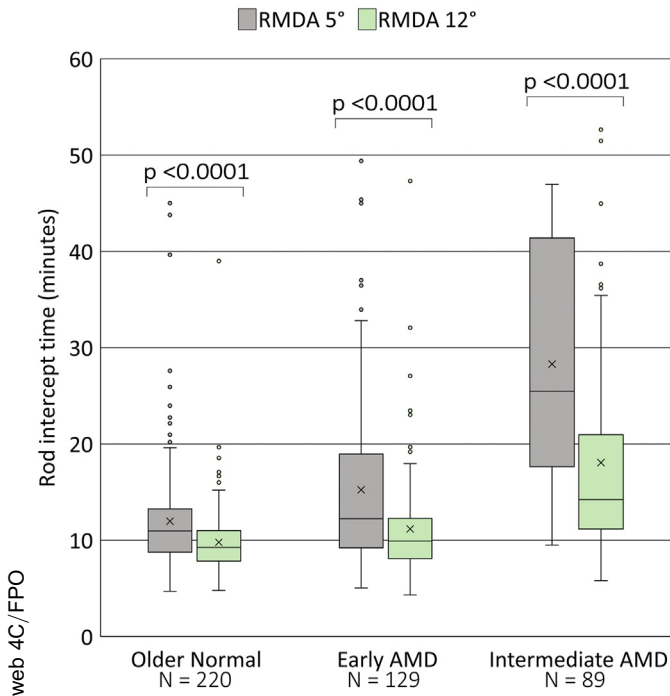


**Figure 3.** Box plots comparing the distributions of rod intercept time (RIT) at 5° and 12° stratified by Age-Related Eye Disease Study (AREDS) 9-step age-related macular degeneration (AMD) severity. Note that RIT is greater at 5° than at 12° in each disease severity group, meaning that the rate of rod-mediated dark adaptation (RMDA) is slower at 5°. Rod intercept time at 5° was set to 45 minutes for 1 eye in normal macular health, 1 eye with early AMD and 13 eyes with intermediate AMD. At 12°, RIT was set to 45 minutes for 2 eyes with intermediate AMD. Outliers are values 1.5 times the inter-quartile range below quartile 1 and above quartile 3. This is also the case in Figs S4–S6.

Fig S4 using the AREDS 9-step system, and available at <https://www.opthalmologyscience.org>. Note that a major difference in the Beckman system compared to the AREDS 9-step system, as applied to this cohort, is that the Beckman system decreases the number of eyes graded as early AMD and increases the number of eyes graded as intermediate AMD. In our sample, for the AREDS 9-step system, there were 129 early AMD eyes, whereas in the Beckman there are only 87, due to 42 eyes moving to the intermediate AMD category in Beckman. For eyes classified by the Beckman and tested at 5°, RIT is higher in early and intermediate AMD for SDD as compared to no SDD. This result is similar to the result for the AREDS 9-step classification system in Fig S4 (available at <https://www.opthalmologyscience.org>). At 12°, RIT in eyes with SDD is longer than in eyes without SDD, for intermediate AMD only, with no differences in normal aging and early AMD. This result is similar to the AREDS 9-step result in Fig S4 (available at <https://www.opthalmologyscience.org>).

## Discussion

In this large sample of well-characterized participants, we find that RMDA rate assessed at 5° differs more between

normal aging to intermediate AMD than RMDA rate assessed at 12°. Others<sup>12,13,22,23</sup> have also found slower RMDA at 5° in AMD as compared to more eccentric locations (also summarized in<sup>42</sup>). We probed RMDA in relation to photoreceptor topography and current models of deposit-driven AMD progression (Fig 1). At 5° SDD deposits typically are absent until well into AMD progression. They first appear near the superior arcades and spread toward the fovea without covering it. As developed below, these seemingly counterintuitive findings for SDD-bearing eyes most likely result from processes leading to and resulting from soft drusen under the fovea, which begins earlier in life than SDD.<sup>43,44</sup> Our results have ramifications for the design of clinical trials and observational studies. Regional specificity of RMDA, along with information about study design, intervention type, and intervention mechanism of action can lead to efficient clinical trials for a disease that is both prevalent and lacking a targeted treatment.

Our focus on the interface of aging and AMD is a powerful approach for probing disease mechanisms prior to secondary effects in atrophy like intense gliosis.<sup>45</sup> Further, using retinal eccentricity is also powerful, because of the wide range and steep gradients of cone and rod densities in human macula (Fig 1B). Cone photoreceptor density peaks in the foveal central bouquet (at 0°) and decreases by 10-fold by ~3.5° (1 mm). Rods appear at ~0.6° (0.175 mm) from the fovea and increase to a maximum like that of cones (~150 000/mm<sup>2</sup>) at 10.4° to 17.4° (3–5 mm), in an elliptical ring at the vascular arcades that also surrounds the optic nerve head. The inner slope of the rod ring (including 5°) is proportionately more affected by cell loss in aging than the crest of the ring (at 12°). Tests of visual function thus provide an opportunity to assess mechanisms underlying the vulnerability of parafoveal rods, in the context of resilient foveal cones.

In layered outer retina, and assuming a largely monotonic progression sequence (i.e., always getting worse with time), disease at any one time point is most severe in the layer where it started first. Extracellular deposits (soft drusen, SDD) generally expand over time, yet a small portion disappear without atrophy, and together these represent daily variation in cellular activities. Based on large effect sizes in aging, degeneration of choriocapillaris endothelium and lipidation of Bruch's membrane (BrM) are strong candidates for initial site of degeneration, impacting the transfer of constitutively produced materials to and from the choroidal circulation. By histochemistry, the "Oil Spill in BrM" under the fovea starts with lipoprotein deposition in late adolescence, becoming visible clinically later.<sup>43,44</sup> It unfolds throughout adulthood to manifest as soft drusen and basal linear deposit in eyes > 60 years.

Like drusen, SDD have a lifespan trajectory, and it is incompletely described to date. By histology they can occur in eyes with insufficient RPE degeneration to meet criteria for AMD.<sup>25</sup> Patients with SDD are often reported as older than patients without them,<sup>46,47</sup> as we also found in this study. Interestingly, a common SDD progression pathway is neovascularization of retinal origin (type 3, or retinal angiomatous proliferation).<sup>48</sup> Like the slowest RMDA

Table 2. RIT Stratified by AMD Severity Group for Test Targets Presented at 5° and 12°

Test Target Location	Normal Macular Health Early AMD Intermediate AMD			P-Values			
	Mean (SD)	Mean (SD)	Mean (SD)	Overall	Normal vs Early	Normal vs Intermediate	Early vs Intermediate
All eyes	N = 220	N = 129	N = 89				
5° RIT	12.0 (5.5)	15.2 (9.2)	28.3 (11.9)	< 0.0001	0.0008	< 0.0001	< 0.0001
12° RIT	9.8 (3.2)	11.2 (5.4)	18.1 (10.6)	< 0.0001	0.0678	< 0.0001	< 0.0001
Eyes without SDD	N = 200	N = 97	N = 48				
5° RIT	11.8 (5.0)	14.1 (7.7)	23.8 (10.3)	< 0.0001	0.0091	< 0.0001	< 0.0001
12° RIT	9.7 (2.6)	10.9 (5.7)	13.5 (4.6)	< 0.0001	0.0146	< 0.0001	0.0032
Eyes with SDD	N = 20	N = 32	N = 41				
5° RIT	13.5 (9.0)	18.7 (12.0)	33.6 (11.4)	< 0.0001	0.0848	< 0.0001	< 0.0001
12° RIT	11.1 (7.0)	12.0 (4.7)	23.4 (13.0)	< 0.0001	0.7484	< 0.0001	< 0.0001

Results are stratified by SDD presence. Comparisons are age-adjusted. AMD = age-related macular degeneration; RIT = rod intercept time; SD = standard deviation; SDD = subretinal drusenoid deposit.

rates, type 3 neovascularization also occurs close to the fovea, i.e., not near the SDD themselves, and typically in conjunction with large soft drusen.<sup>49–51</sup> One could envision a scenario in which SDD occur in the setting of the same vascular insufficiency (i.e., choriocapillaris and BrM failure) that led to drusen. Notably, SDD are not specific to AMD but also occur in diseases with BrM pathology and deposition of aberrant RPE basal lamina material,<sup>52,53</sup> where delayed RMDA also occurs.<sup>54,55</sup>

The model in Figure 1 potentially explains the spatial dissonance between SDD, visual consequences, and sequelae. In brief, we hypothesize that soft drusen preferentially cluster under the fovea<sup>28,56</sup> due to a highly focused area of lipid transfer on top of age-related dysfunction of choriocapillary endothelium and BrM that collectively impairs transfer to and from the circulation. The RMDA 5° test location lies on the perimeter of this region in the inner ring of the ETDRS grid. This location could be affected by both deposits, yet by the reasoning above, it is affected by drusen-related processes before it is affected by SDD-related processes. Lipid transfer is focused at the fovea, because xanthophyll carotenoid pigments are highly concentrated in foveal neurons and Müller glia and are replenished by diet.<sup>57</sup> After taking up plasma high-density lipoprotein and low-density lipoprotein and transferring carotenoids to the neurosensory retina,<sup>58,59</sup> RPE releases unneeded lipids back to the circulation in its own large cholesteryl ester-rich lipoproteins.<sup>60</sup> These accumulate in, then on, BrM as soft drusen material. Hypoxia ensues due to RPE elevation, and component lipids become peroxidized and pro-inflammatory. To date, limited evidence indicates that inflammation associated with SDD occurs well into AMD. In our model, rods are vulnerable because they depend on the choriocapillaris. Cones are sustained by xanthophyll-enriched glia and glial access to the retinal vasculature. Deposit-driven progression is best explained by an early transport failure across the choriocapillaris and BrM (“floor of microangiopathy”)<sup>61</sup>. As disease continues, we also suspect changes in uptake and transfer functions of RPE. Our previous OCT analysis<sup>18</sup> showed that pixels on either side of the RPE-basal lamina-BrM band were highly predictive of RIT.

Selection of RMDA as an outcome measure in AMD should consider these issues. Our finding that RMDA is slower at 5° than at 12° agrees with previous findings of long RIT near the fovea.<sup>12,13,22,23</sup> Thus, testing at 12° takes less time and may be preferred if protocol length is the primary consideration. Yet we emphasize that effect size is much bigger at 5° than 12° in all groups. For example, comparing intermediate AMD to older normal eyes, the effect size for RMDA 12° is 8.3 minutes, but it is double (16.3 minutes) for RMDA 5°. This is also true when comparing early AMD versus normal eyes. These effect sizes become even larger for eyes with SDD (20.1 minutes for 5° and 12.3 minutes for 12°). A larger effect size engenders higher statistical power in evaluating hypotheses, while also implying a smaller sample. Thus, in comparing AMD eyes to normal eyes, RIT can be achieved more quickly at 12° than at 5° but at the cost of halving the effect size. In turn, choosing 12° may increase the number of patients, the length of a trial, or both. Another consideration is that observer responses for non-foveal targets involve more fixation errors.<sup>62,63</sup> This was borne out in our study where 10.6% of participants had invalid RMDA data at 12° (> 30% fixation errors) and only 6.9% had invalid data at 5°.

We stratified eyes using a color fundus photography grading system (AREDS 9-step), which is reliable in our hands and compatible with our published and forthcoming data. Notably, we obtained consistent results with both AREDS<sup>32</sup> and Beckman<sup>33</sup> grading systems, despite the fact that the number of eyes considered early AMD differed between the 2 stratifications (N = 129 eyes for AREDS; N = 87 for Beckman). We attribute this shift to eyes with pigmentary changes only (without drusen) being considered early AMD in AREDS and intermediate AMD in Beckman. Of note, AREDS includes a mechanism for SDD bookkeeping but does not consider them in the final grade; Beckman does not mention SDD at all. The absence of SDD in AMD classification systems, particularly for the Beckman system, created at a time when histologic correlates indeed had either already been offered or were forthcoming,<sup>30,64</sup> is clearly a limit to understanding AMD disease severity. The AREDS and Beckman systems were developed for different

purposes (progression versus consensus), a full explication of which is beyond our current scope. A standardized multimodal imaging for AMD onset and progression does not yet exist. The ALSTAR2 imaging dataset may be useful for generating a system in the future.

A strength of the study is a large sample of eyes (N = 438) designed to focus on the emergence of AMD, an infrequently studied disease stage in AMD research. The study design incorporated precise measures of macular photoreceptor topography and a model of deposit-driven progression. Thus, we assessed locations with distinct cellular content, aging changes, and predominant pathology. A relatively new imaging approach incorporating *en face* OCT was used to identify eyes with SDD. Limitations include the predominance of participants of European descent, the testing of only 2 retinal locations, and the lack of functional assessment of retina overlying specific deposits. Graders who independently evaluated the presence of SDD may have missed SDD identification in some

situations, although the agreement between graders was strong.

Ideally, clinical trial outcomes should meaningfully impact vision by preventing, halting, or reversing the disease process and visual decline. This goal is achievable with assessments (functional or structural) that reflect how treatments modify causal pathways in AMD progression.<sup>65,66</sup> We believe that RMDA has potential of being such a test. We emphasize that our study design is cross-sectional and thus offers insight rather than measured disease progression. However, strong results from the baseline cohort support the overall conceptual framework of ALSTAR2,<sup>67</sup> which will be tested further at follow-up. The remarkable geometry of photoreceptors and their support cells, and diagnostic technologies like OCT, RMDA, and others in development, allows visualizable interrogation of cells in action, over time. One can imagine a 4-D puzzle being deciphered by investigators worldwide.<sup>68</sup>

## Footnotes and Disclosures

Originally received: August 18, 2022.

Final revision: January 16, 2023.

Accepted: January 17, 2023.

Available online: January 23, 2023. Manuscript no. XOPS-D-22-00183

<sup>1</sup> Department of Ophthalmology & Visual Sciences, Heersink School of Medicine, University of Alabama at Birmingham, Birmingham, Alabama.

<sup>2</sup> Department of Epidemiology, School of Public Health, University of Alabama at Birmingham, Birmingham, Alabama.

Disclosure(s):

All authors have completed and submitted the ICMJE disclosures form.

The authors made the following disclosures:

C.O.: Inventor on the device used to measure dark adaptation in this study; Consultant—Johnson & Johnson Vision (outside this work).

C.A.C.: Research support—Genentech, Roche, Regeneron, and Heidelberg Engineering; Consultant—Apellis and Boehringer Ingelheim (all outside this work).

Supported by the National Institutes of Health grants R01EY029595 (C.O., C.A.C.), R01EY027948, and P30EY03039, EyeSight Foundation of Alabama, Dorsett Davis Discovery Fund, Alfreda J. Schueler Trust, Research to Prevent Blindness, and Heidelberg Engineering (C.A.C.).

HUMAN SUBJECTS: The study was approved by the Institutional Review Board of the University of Alabama at Birmingham. All participants provided written informed consent after the nature and purpose of the study were explained. Conduct of the study followed the Declaration of Helsinki.

Author Contributions:

Research design: Owsley, McGwin, Curcio

Data Acquisition and research execution: Owsley, Swain, McGwin, Clark, Kar, Curcio

Data analysis and interpretation: Owsley, Swain, McGwin, Clark, Kar, Curcio

Obtained funding: Owsley, Curcio, McGwin

Manuscript preparation: Owsley, Swain, McGwin, Clark, Kar, Curcio

Abbreviations and Acronyms:

**ALSTAR2** = Alabama Study on Early Age-Related Macular Degeneration 2; **AMD** = age-related macular degeneration; **AREDS** = Age-Related Eye Disease Study; **BrM** = Bruch's membrane; **RIT** = rod intercept time; **RMDA** = rod-mediated dark adaptation; **RPE** = retinal pigment epithelium; **SDD** = subretinal drusenoid deposit.

Keywords:

Normal aging, Rod-mediated dark adaptation, Drusen, Subretinal drusenoid deposits, Age-related macular degeneration.

Correspondence:

Cynthia Owsley, PhD, MSPH, Department of Ophthalmology & Visual Sciences, Heersink School of Medicine, University of Alabama at Birmingham, 1720 University Blvd., Suite 609, Birmingham AL 35294-0009  
E-mail: [cynthiaowsley@uabmc.edu](mailto:cynthiaowsley@uabmc.edu).

## References

- Jaffe GJ, Westby K, Csaky KG, et al. C5 inhibitor avacincaptad pegol for geographic atrophy due to age-related macular degeneration: a randomized pivotal phase 2/3 trial. *Ophthalmology*. 2021;128:576–586.
- Liao DS, Grossi FV, El Mehdi D, et al. Complement C3 inhibitor pegcetacoplan for geographic atrophy secondary to age-related macular degeneration: a randomized phase 2 trial. *Ophthalmology*. 2020;127:186–195.
- Nittala MG, Metlapally R, Ip M, et al. Association of pegcetacoplan with progression of incomplete retinal pigment epithelium and outer retinal atrophy in age-related macular degeneration: a post hoc analysis of the FILLY randomized trial. *JAMA Ophthalmol*. 2022;140:243–249.
- Steinmetz RL, Haimovici R, Jubb C, et al. Symptomatic abnormalities of dark adaptation in patients with age-related Bruch's membrane change. *Br J Ophthalmol*. 1993;77:549–554.
- Owsley C, Jackson GR, White MF, et al. Delays in rod-mediated dark adaptation in early age-related maculopathy. *Ophthalmology*. 2001;108:1196–1202.

6. Owsley C, McGwin G, Jackson G, et al. Cone- and rod-mediated dark adaptation impairment in age-related maculopathy. *Ophthalmology*. 2007;114:1728–1735.
7. Flamendorf J, Agrón E, Wong WT, et al. Impairments in dark adaptation are associated with age-related macular degeneration severity and reticular pseudodrusen. *Ophthalmology*. 2015;122:2053–2062.
8. Sevilla MB, McGwin GJ, Lad EM, et al. Relating retinal morphology and function in aging and early to intermediate age-related macular degeneration subjects. *Am J Ophthalmol*. 2016;165:65–77.
9. Lains I, Miller JB, Park DH, et al. Structural changes associated with delayed dark adaptation in age-related macular degeneration. *Ophthalmology*. 2017;124:1340–1352.
10. Cocce KJ, Stinnett SS, Luhmann UFO, et al. Visual function metrics in early and intermediate dry age-related macular degeneration for use as clinical trial endpoints. *Am J Ophthalmol*. 2018;189:127–138.
11. Lains I, Park DH, Mukai R, et al. Peripheral changes associated with delayed dark adaptation in age-related macular degeneration. *Am J Ophthalmol*. 2018;190:113–124.
12. Tahir HJ, Rodrigo-Diaz E, Parry NRA, et al. Slowed dark adaptation in early AMD: dual stimulus reveals scotopic and photopic abnormalities. *Invest Ophthalmol Vis Sci*. 2018;59:AMD202–AMD210.
13. Tan RS, Guymer RH, Aung K-Z, et al. Longitudinal assessment of rod function in intermediate age-related macular degeneration with and without reticular pseudodrusen. *Invest Ophthalmol Vis Sci*. 2019;60:1511–1518.
14. Echols BS, Clark ME, Swain TA, et al. Hyperreflective foci and specks are associated with delayed rod-mediated dark adaptation in nonneovascular age-related macular degeneration. *Ophthalmol Retina*. 2020;4:1059–1068.
15. Kar D, Clark ME, Swain TA, et al. Local abundance of macular xanthophyll pigment is associated with rod- and cone-mediated vision in aging and age-related macular degeneration. *Invest Ophthalmol Vis Sci*. 2020;61:46.
16. Lains I, Pundlik SJ, Nigalye A, et al. Baseline predictors associated with 3-year changes in dark adaptation in age-related macular degeneration. *Retina*. 2021;41:2098–2105.
17. Guymer RH, Tan RS, Luu CD. Comparison of visual function tests in intermediate age-related macular degeneration. *Transl Vis Sci Technol*. 2021;10:14.
18. Lee AY, Lee CS, Blazes MS, et al. Exploring a structural basis for delayed rod-mediated dark adaptation in age-related macular degeneration via deep learning. *Transl Vis Sci Technol*. 2020;9:62.
19. Owsley C, McGwin Jr G, Clark ME, et al. Delayed rod-mediated dark adaptation is a functional biomarker for incident early age-related macular degeneration. *Ophthalmology*. 2016;123:344–351.
20. Owsley C, Clark ME, Huisingh CE, et al. Visual function in older eyes in normal macular health: association with incident early age-related macular degeneration 3 years later. *Invest Ophthalmol Vis Sci*. 2016;57:1782–1789.
21. Mullins RF, McGwin Jr G, Searcey K, et al. The ARMS2 A69S polymorphism is associated with delayed rod-mediated dark adaptation in eyes at risk for incident age-related macular degeneration. *Ophthalmology*. 2018;126:591–600.
22. Flynn OJ, Jeffrey BG, Cukras CA. Characterization of rod function phenotypes across a range of age-related macular degeneration severities and subretinal drusenoid deposits. *Invest Ophthalmol Vis Sci*. 2018;59:2411–2421.
23. Binns AM, Taylor DJ, Edwards LA, Crabb DP. Determining optimal test parameters for assessing dark adaptation in people with intermediate age-related macular degeneration. *Invest Ophthalmol Vis Sci*. 2018;59:AMD114–AMD121.
24. Wu Z, Fletcher EL, Kumar H, et al. Reticular pseudodrusen: a critical phenotype in age-related macular degeneration. *Prog Retin Eye Res*. 2021;88:101017.
25. Chen L, Messinger JD, Kar D, et al. Biometric, impact, and significance of basal linear deposit and subretinal drusenoid deposit in age-related macular degeneration. *Invest Ophthalmol Vis Sci*. 2021;62:33.
26. Curcio CA, Sloan KR, Kalina RE, Hendrickson AE. Human photoreceptor topography. *J Comp Neurol*. 1990;292:497–523.
27. Ach T, Huisingh C, McGwin Jr G, et al. Quantitative autofluorescence and cell density maps of the human retinal pigment epithelium. *Invest Ophthalmol Vis Sci*. 2014;55:4832–4841.
28. Wang JJ, Rochtchina E, Lee AJ, et al. Ten-year incidence and progression of age-related maculopathy: the Blue Mountains Eye study. *Ophthalmology*. 2007;114:92–98.
29. Snodderly DM, Auran JD, Delori FC. The macular pigment. II. Spatial distribution in primate retinas. *Invest Ophthalmol Vis Sci*. 1984;25:674–685.
30. Curcio CA, Messinger JD, Sloan KR, et al. Subretinal drusenoid deposits in non-neovascular age-related macular degeneration: morphology, prevalence, topography, and biogenesis model. *Retina*. 2013;33:265–276.
31. Spaide RF. Improving the age-related macular degeneration construct: a new classification system. *Retina*. 2018;38:891–899.
32. Age-Related Eye Disease Study Research Group. The Age-Related Eye Disease Study severity scale for age-related macular degeneration. AREDS Report No. 17. *Arch Ophthalmol*. 2005;123:1484–1498.
33. Ferris FLI, Wilkinson CP, Bird A, et al. Clinical classification of age-related macular degeneration. *Ophthalmology*. 2013;120:844–851.
34. Curcio CA, Millican CL, Allen KA, Kalina RE. Aging of the human photoreceptor mosaic: evidence for selective vulnerability of rods in central retina. *Invest Ophthalmol Vis Sci*. 1993;34:3278–3296.
35. Curcio CA, Medeiros NE, Millican CL. Photoreceptor loss in age-related macular degeneration. *Invest Ophthalmol Vis Sci*. 1996;37:1236–1249.
36. Pugh ENJ. Rushton's paradox: rod dark adaptation after flash photolysis. *J Physiol*. 1975;248:413–431.
37. Jackson GR, Edwards JG. A short-duration dark adaptation protocol for assessment of age-related maculopathy. *J Ocul Biol Dis Infor*. 2008;1:7–11.
38. Lamb TD, Pugh ENJ. Dark adaptation and the retinoid cycle of vision. *Prog Retin Eye Res*. 2004;23:307–380.
39. Leibrock CS, Reuter T, Lamb TD. Molecular basis of dark adaptation in rod photoreceptors. *Eye*. 1998;12:511–520.
40. Owsley C, Swain TA, McGwin G, et al. How vision is impaired from aging to early and intermediate age-related macular degeneration: insights from ALSTAR2 baseline. *Transl Vis Sci Technol*. 2022;11:17.
41. Zweifel SA, Spaide RF, Curcio CA, et al. Reticular pseudodrusen are subretinal drusenoid deposits. *Ophthalmology*. 2010;117:303–312.
42. Nigalye A, Hess K, Pundlik S, et al. Dark adaptation and its role in age-related macular degeneration. *J Clin Med*. 2022;11:1358.
43. Pauleikhoff D, Harper C, Marshall J, Bird A. Aging changes in Bruch's membrane. A histochemical and morphologic study. *Ophthalmology*. 1990;97:171–178.
44. Curcio CA, Millican CL, Bailey T, Kruth H. Accumulation of cholesterol with age in human Bruch's membrane. *Invest Ophthalmol Vis Sci*. 2001;42:265–274.

45. Edwards MM, McLeod DS, Bhutto IA, et al. Subretinal glial membranes in eyes with geographic atrophy. *Invest Ophthalmol Vis Sci.* 2017;58:1352–1367.
46. Zhou Q, Daniel E, Maguire MG, et al. Pseudodrusen and incidence of late age-related macular degeneration in fellow eyes in the CAPT Trials. *Ophthalmology.* 2016;123:1530–1540.
47. Buitendijk GHS, Hooghard AJ, Brussee C, et al. Epidemiology of reticular pseudodrusen in age-related macular degeneration: the Rotterdam Study. *Invest Ophthalmol Vis Sci.* 2016;57:5593–5601.
48. Tsai AS, Cheung N, Gan AT, et al. Retinal angiomatic proliferation. *Surv Ophthalmol.* 2017;62:462–492.
49. Su D, Lin S, Phasukkijwatana N, et al. An updated staging system of type 3 neovascularization using spectral domain optical coherence tomography. *Retina.* 2016;36 supplement 1: S40–S49.
50. Sarks JP, Sarks SH, Killingsworth MC. Evolution of soft drusen in age-related macular degeneration. *Eye.* 1994;8: 269–283.
51. Balaratnasingam C, Messenger JD, Sloan KR, et al. Histologic and optical coherence tomography correlations in drusenoid pigment epithelium detachment in age-related macular degeneration. *Ophthalmology.* 2017;124:644–645.
52. Gliem M, Muller PL, Mangold E, et al. Reticular pseudodrusen in Sorsby Fundus Dystrophy. *Ophthalmology.* 2015;122:1555–1562.
53. Gliem M, Hendig D, Finger RP, et al. Reticular pseudodrusen associated with a diseased Bruch membrane in pseudoxanthoma elasticum. *JAMA Ophthalmol.* 2015;133: 581–588.
54. Steinmetz R, Polkinghorne P, Fitzke F, et al. Abnormal dark adaptation and rhodopsin kinetics in Sorsby's Fundus Dystrophy. *Invest Ophthalmol Vis Sci.* 1992;33:1633–1636.
55. Hess K, Gliem M, Birtel J, et al. Impaired dark adaptation associated with a diseased bruch membrane in pseudoxanthoma elasticum. *Retina.* 2020;40:1988–1995.
56. Joachim N, Mitchell P, Burlutsky G, et al. The incidence and progression of age-related macular degeneration over 15 years: the Blue Mountain Eye Study. *Ophthalmology.* 2015;122: 2482–2489.
57. Curcio CA. Antecedents of soft drusen, the specific deposit of age-related macular degeneration, in the biology of human macula. *Invest Ophthalmol Vis Sci.* 2018;59:AMD182–AMD194.
58. Thomas SE, Harrison EH. Mechanisms of selective delivery of xanthophylls to retinal pigment epithelial cells by human lipoproteins. *J Lipid Res.* 2016;57:1865–1878.
59. Vachali PP, Besch BM, Gonzalez-Fernandez F, Bernstein PS. Carotenoids as possible interphotoreceptor retinoid-binding protein (IRBP) ligands: a surface plasmon resonance (SPR) based study. *Arch Biochem Biophys.* 2013;539:181–186.
60. Curcio CA, Johnson M, Huang JD, Rudolf M. Aging, age-related macular degeneration, and the response-to-retention of apolipoprotein B-containing lipoproteins. *Prog Retin Eye Res.* 2009;28:393–422.
61. Fleckenstein M, Keenan TDL, Guymer RH, et al. Age-related macular degeneration. *Nat Rev Dis Primers.* 2021;7:31.
62. Carrasco M, Evert DL, Chang I, Katz SM. The Eccentricity effect: target eccentricity affects performance on conjunction searches. *Percept Psychophys.* 1995;57:1241–1261.
63. Wall M, Johnson CA. Morphology and repeatability of automated perimetry using stimulus sizes III, V, and VI. *Med Res Arch.* 2020;9:1–15.
64. Sarks J, Arnold J, Ho IV, et al. Evolution of reticular pseudodrusen. *Br J Ophthalmol.* 2011;95:979–985.
65. Schaal KB, Rosenfeld PJ, Gregori G, et al. Anatomic clinical trial endpoints for nonexudative age-related macular degeneration. *Ophthalmology.* 2016;123:1060–1079.
66. Wu Z, Guymer RH. Can the onset of atropic age-related macular degeneration be an acceptable endpoint for preventative trials? *Ophthalmologica.* 2020;243:399–403.
67. Curcio CA, McGwin Jr G, Sadda SR, et al. Functionally validated imaging endpoints in the Alabama study on early age-related macular degeneration 2 (ALSTAR2): design and methods. *BMC Ophthalmol.* 2020;20:196.
68. Miller JW. Age-related macular degeneration revisited – piecing the puzzle: the LXIX Edward Jackson Memorial Lecture. *Am J Ophthalmol.* 2013;155:1–35.e13.